

# Design and Numerical Study of Hydrokinetic Turbines at Bakaru Hydropower Tail Race for the Application of Combined-Cycle Hydropower Systems

Muhammad Ramadhan\*, I Nengah Diasta & Gea Fardias Mu'min

Faculty of Mechanical and Aerospace Engineering, Institut Teknologi Bandung,  
Jalan Ganesa 10, Bandung 40132, Indonesia

\*Email: muh.ramadhan295@pln.co.id

**Abstract.** The Net Zero Emission (NZE) target for 2060 has driven countries to increase the number of renewable energy power plants. In addition to building new renewable power plants, there is also an effort to enhance the capacity or optimize existing renewable power plants. One such optimization is the utilization of kinetic energy in the tail race of HEPP, which can be harnessed to generate electricity by installing a hydrokinetic turbine. The electricity generated from the tail race can be fed into the grid for network consumption or used to power auxiliary equipment at the hydroelectric plant. This reduces the self-consumption (PS) of the plant, a concept known as Combined-Cycle Hydropower Systems. Bakaru Hydro Electric Power Plant (HEPP) is a run-of-river hydroelectric power plant equipped with Francis vertical turbines, located in Bakaru Village, Lembang District, South Sulawesi. flow speed measurements of the tail race at Bakaru HEPP, using an Acoustic Doppler Current Profiler (ADCP), showed flow speeds ranging from 1.6 m/s to 2.4 m/s during maximum load conditions of 126 MW. Therefore, the theoretical power that can be generated by the hydrokinetic turbine is approximately 48 kW. It is important to determine the optimal placement of the turbine to maximize the utilization of water flow in the tail race and minimize the impact caused by the turbine installation. Therefore, this study designs three turbines with different blade lengths based on solidity (0.1, 0.2, and 0.3). The chord variation is 100 mm, 209 mm, and 314 mm, and simulates their placement in two different positions in the tailrace to analyze the effect on the performance of the hydrokinetic turbine.

**Keywords:** *Combined-cycle hydropower systems, hydrokinetics turbine, tailrace, hydropower plant.*

## 1 Introduction

Hydropower is one of the largest renewable energy potentials that has been exploited, where hydropower contributes around 20 percent of the total electrical energy in the world [1].

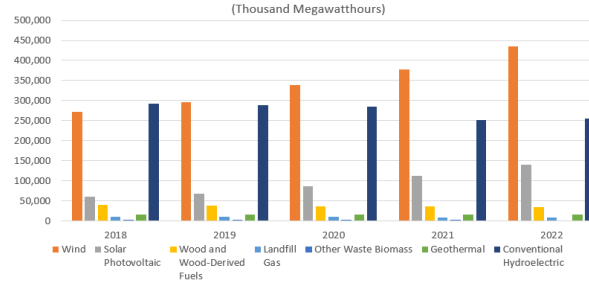


**Figure 1** Energy generation from various renewable energy sources [2]

The use of hydropower plants continues to be developed because hydropower can produce electricity without pollution, the average annual growth in hydropower use is 22 GW[3]. The use of hydropower supports the country's commitment to achieving net zero emissions (NZE), which is a response to global climate change by reducing carbon emissions to achieve the global warming target of 1.5°C based on the Paris Agreement, where developing countries have an NZE target in 2050 [4].

Besides creating new power plants, increasing renewable energy can also be done by optimizing hydropower plants that are already operating by installing hydrokinetic turbines in their tail race, and can be utilized for supply their own consumption which is called a Combined-Cycle Hydropower System [5].

The amount of power that can be generated from the tail race can be seen from its correlation with the existing hydropower head.

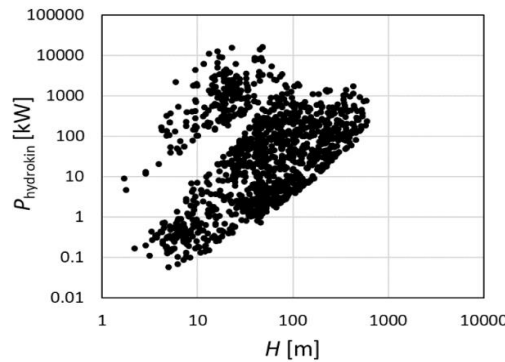


**Figure 2** The effect of head on the energy that can be taken from the tail race [5]

## 2. Literature Review

### 2.1 Bakaru Hydropower Plant

The Bakaru hydroelectric power plant is a Run of River (RoR) type which use the flow of Mamasa river in Ulusaddang village, Lembang subdistrict, Pinrang Regency, South Sulawesi. It is located 280 km north of Makassar city. Bakaru hydropower specifications can be seen in Table 1.1 below:

**Table 1.1** Specifications of Bakaru Hydroelectric Power Plant

1	Type	Run Off River
2	Turbine	Francis Vertical
3	Maximum Discharge	45 m <sup>3</sup> /sec
4	Effective Head	322.20 m
5	Maximum Output	126 MW
6	Annual Generated Energy	1030 GWH
7	Catchment	1080 Km <sup>2</sup>

One of the waterway part at the Bakaru hydroelectric power plant is the tail race, its functions is streaming water from the draft tube back to the river flow. The Bakarus tail race specification can be seen at Table 1.2 below.



**Figure 3** Tail race at Bakaru HEPP

**Table 1.2** Specification of Bakaru HEPP tail race

No	Dimensi	Satuan
1.	Width Tail Race Outlet	6 meters
2.	Water Depth	± 4 meters (EL. 281 s.d HWL 284)
3.	Flow (Q)	1 Unit operating = 22,5 m <sup>3</sup> /s 2 Unit operating = 45,0 m <sup>3</sup> /s

### 2.2 Hydrokinetic Turbine (HDKT)

Utilization of water energy in HDKT is extracted from kinetic energy of water flow. HDKT is “zero-head” hydroelectric power plants, their operating principle

is similar to wind turbines. HDKT is often easier to implement because it generally does not require high-cost civil engineering work compared to conventional hydroelectric power plants [13]. The following is the theoretical power potential equation that can be taken from an HDKT [7]:

$$P_{\text{HKT}} = \frac{1}{2} \rho A V^3 \quad (1)$$

Where  $\rho$  is the fluid density ( $\text{kg/m}^3$ ),  $A$  is the HDKT swept area ( $\text{m}^2$ ),  $V$  is the fluid velocity ( $\text{m/s}$ ), and  $P_{\text{HKT}}$  is the HDKT theoretical power ( $\text{W}$ ). Of course, the theoretical power cannot be fully realized due to efficiency and also restrictions imposed by Betz's law, which is a maximum of 0.59 [8][9]. The type of HDKT used also affects efficiency as shown in the following table.

**Table 2.2** Mechanical Power Efficiency of Hydrokinetic Turbines [10]

HDKT	Efficiency	Flow velocity
gaman	15% - 18%	>0.5 m/s
Tyson	16%	>0.5 m/s
Savonius	19%	>2 m/s
Seaflow	20%	>2 m/s
Darrieus	23%	>2 m/s
Gorlov	35%	>0.6 m/s

### 2.3 Computational Fluid Dynamic

Computational Fluid Dynamics (CFD) is a science used to predict fluid flow, heat transfer, chemical reactions and other phenomena based on mathematical equations that represent the laws of conservation of mass, momentum and energy. In general, the CFD simulation process is divided into three stages:

1. Pre-processing which includes geometry assembly and meshing processes.
2. Solving which includes determining the model, determining boundary conditions, and iteration.
3. Post-processing which includes the solution analysis process and visualization analysis.

There are various mathematical models that can be used in CFD, the turbulence model that will be used is determined based on several things such as the level of accuracy, computing resources and the available time.

Based on several literatures, the most frequently used in turbine simulations are k-epsilon and k-omega, k-omega is more accurate when taking into account near-wall interactions, apart from that, the SST mode in k-omega is also chosen, which

is a mode that has been developed for flow simulations on the airfoil. The specific dissipation rate ( $\omega$ ) and the turbulence kinetic energy ( $k$ ) are obtained from the following transport equations [6].

$$\frac{\partial}{\partial t}(\rho k) + \frac{\partial}{\partial x_i}(\rho k u_i) = \frac{\partial}{\partial x_j} \left[ \Gamma_k \frac{\partial k}{\partial x_j} \right] + G_k - Y_k + S_k \quad (2)$$

And for  $\omega$ :

$$\frac{\partial}{\partial t}(\rho \omega) + \frac{\partial}{\partial x_i}(\rho \omega u_i) = \frac{\partial}{\partial x_j} \left[ \Gamma_\omega \frac{\partial \omega}{\partial x_j} \right] + G_\omega - Y_\omega + D_\omega + S_\omega \quad (3)$$

where  $G_\omega$  represents the generation of  $\omega$ ,  $G_k$  represents the generation of  $k$  due to mean velocity gradients,  $\Gamma_k$  and  $\Gamma_\omega$  represent the effective diffusivity of  $k$  and  $\omega$ , respectively.  $Y_\omega$  and  $Y_k$  represent the dissipation of  $\omega$  and  $k$  in the turbulence,  $\delta_\omega$  represents the cross-diffusion term.  $S_\omega$  and  $S_k$  are user-defined source terms.

### 3. METHODOLOGY

#### 3.1 Potential power in tail race of the Bakaru HEPP

By collecting data in 2023, a flow duration curve (FDC) was created, it was found that Q40 – Q100 of the Bakaru Hydroelectric Power Plant was rated at 45 m<sup>3</sup>/s, this is due to the operating pattern of the hydroelectric power plant which is a base load generator, so that the Bakaru Hydroelectric Power Plant has a stable output discharge of 45 m<sup>3</sup>/s at The maximum load is 126 MW, so the flow velocity data taken at the tail race outlet of the Bakaru HEPP when the Hydropower Plant was operating at maximum load.

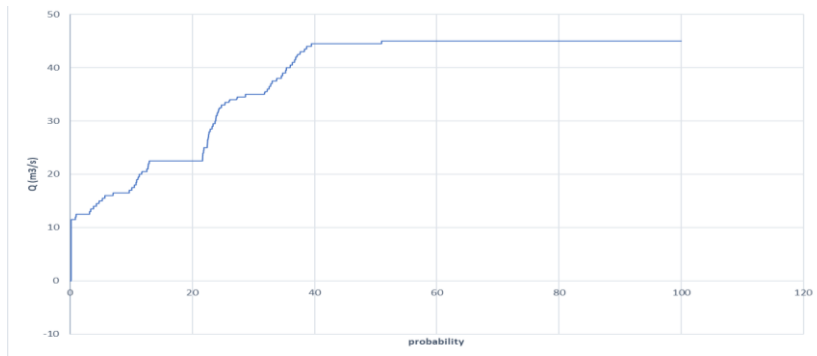


**Figure 4** Flow Duration Curve Bakaru HEPP 2023

From direct measurement using Accoustic Doppler Current Profiler (ADCP). Its found that the mean velocity at the tailrace outlet when the maximum load was 1.9 m/s, so that the potential power that could be generated using equation (1) is 82.3 kW.

## 3.2 HDKT DESIGN

### 3.2.1 Airfoil design

For Gorlov turbines, the blades are made as thin as possible, although this does not significantly affect the turbine output power, it does affect the power coefficient ( $C_p$ ), where in previous research it was found that the optimum airfoil was NACA 0018-64, which has a  $C_{pmax}$  of up to 0.4585 [7].

### 3.2.2 Diameter and height of turbine

The advantage of the helix turbine is that to maintain the swept area of the turbine we can compensate for the decrease in diameter dimensions by increasing the turbine height. Where the turbine height does not affect the centrifugal force on the turbine, so determining the turbine height has no limitations or is only limited by the environmental conditions where the turbine will be used [8]. Therefore, in this study the author maximized the turbine height according to the available space 2 meters. And choose the L/R ratio is two, so the turbine diameter is 1 meters.

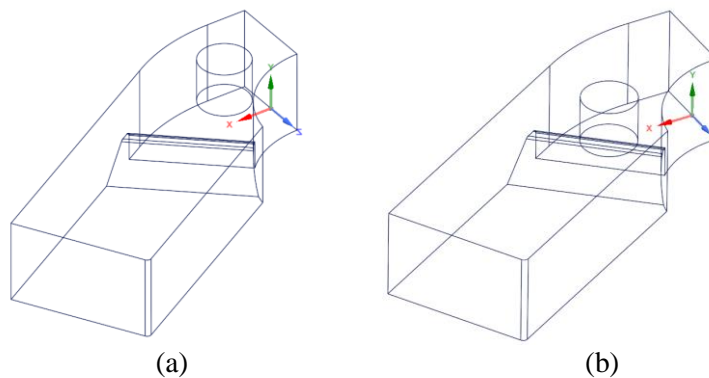


**Figure 5** (a) turbine position 1 (b) turbine position 2

The theoritical power from one turbine can be determined from equation (1), thats are 6.86 kW. Because HKT efficiency is limited by Betz's law at 0.59. so the maximum power potential is 4.05 kW.

### 3.2.3 Amount of turbine blades

From the results of previous research references, it is known that for the same turbine configuration conditions, a hydrokinetic turbine with 3 blades can produce greater output power than a 2 blade hydrokinetic turbine and a 4 blade hydrokinetic turbine [9].

### 3.2.4 Helical pitch angle ( $\phi$ ) & Blade pitch angle

Helical pitch angle ( $\phi$ ) can be calculated with following equation:

$$\phi = \tan^{-1} \left( \frac{nH}{\pi D} \right) \quad (4)$$

$$\phi = \tan^{-1} \left( \frac{3 * 2}{3.14 * 1} \right)$$

$$\phi = 62.37^\circ$$

From the literature it is recommended to use a blade pitch angle with an angle of  $0^\circ$  to  $+2^\circ$ , so in this study a blade angle of  $0^\circ$  or perpendicular to the turbine center line, or parallel to the tangent line was used.

### 3.2.5 Solidity ( $\sigma$ )

In this study, the solidity was varied with values of 0.1, 0.2, and 0.3, so that the chord lengths ( $C$ ) based on the solidity value with following equation are:

$$C = \frac{2\sigma\pi r}{B} \quad (5)$$

**Table 3.1** Chord length variation according solidity value

solidity	Blade amount	phi	radius	chord length	
				m	mm
0.1	3	3.14	0.5	0.1	100
0.2	3	3.14	0.5	0.21	209
0.3	3	3.14	0.5	0.31	314

### 3.2.6 Modelling turbine and tail race

Plotting the Naca 0018 airfoil on airfoiltools.com by inputting the chord length, 100 mm, 210 mm and 314 mm and then import to solidwork. Dimension tail race we adopt from OEM manual book Bakaru HEPP.

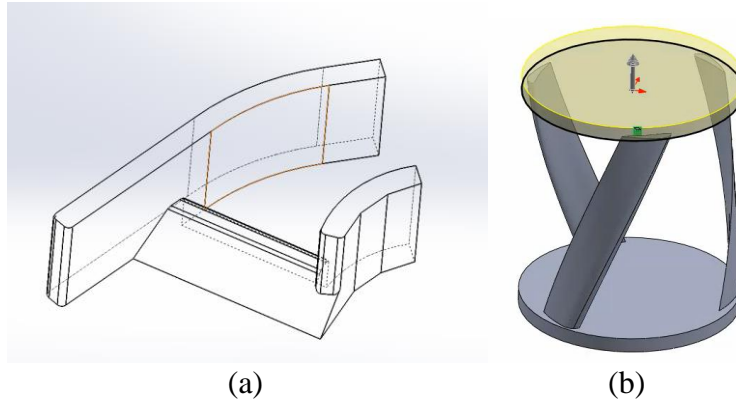


**Figure 6** (a) modelling tail race (b) modelling turbine

### 3.3 CFD

Create a domain for the fluid to be analyzed, in this case we make 3 domain sections, one is turbine domain as rotating domain, two is support domain to make an area which has more meshing, and three is canal domain as stationary domain.

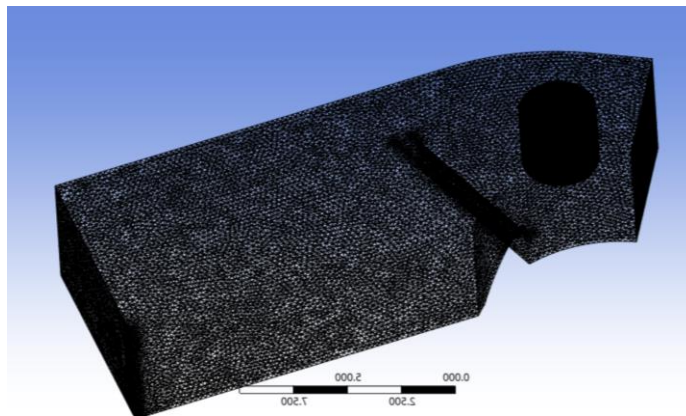


**Figure 7** All domain meshing

The boundaries are set like previous research [7] and in this study the boundaries are set on Table 3.2.

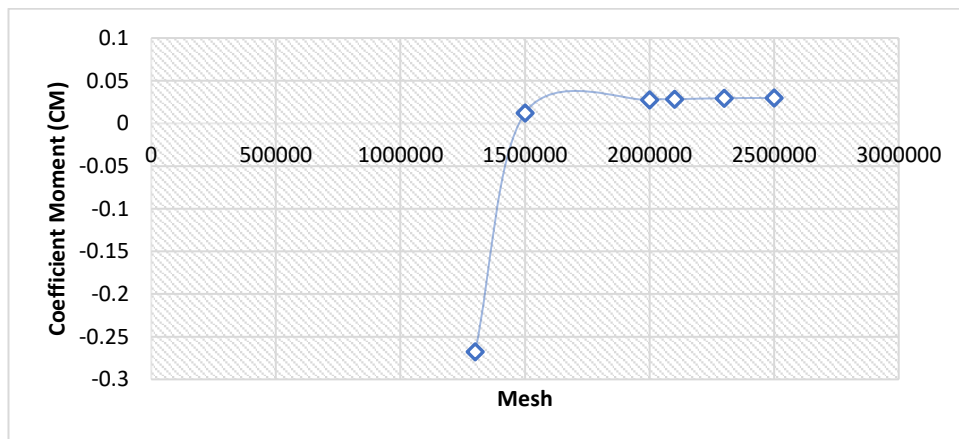


**Table 3.2** Boundary setting

Boundary conditions	Descriptions
Inlet	Flow inlet velocity of 1.9 m/s
outlet	Outflow at atmospheric condition 0 Pa
open	Open at atmospheric condition 0 Pa
top walls as open surface	slip wall
Turbine walls	Rotating with no-slip wall condition
Contact surface of domains	interface

The top wall is defined as the slip-wall to simulate the free surface open-channel flow, whereas the bottom wall is the no-slip boundary [10].

To determine the suitability of the meshing, a mesh independence test is carried out by comparing the number of meshes with the CM (Coefficient moment) value. The error value of the CM from the simulation results is a comparison of the CM results before and after increasing the number of meshes. From the following graph it can be seen the consistency of the CM value starts from meshes above 2 million nodes so for the effectiveness of the simulation the mesh value used is 2100000.

**Figure 8** Graphic mesh vs coefficient moment

The viscous SST k- $\omega$  model the turbulence mode to be used is determined based on several things such as the level of accuracy, computing resources and the amount of time available. Based on several literatures, the most frequently used turbine simulations are k- $\epsilon$  and k- $\omega$ , k- $\omega$  is more accurate when taking into account near-wall interactions, apart from that, the SST mode in k- $\omega$  is also chosen, which is a mode that has been developed for flow simulations. on the airfoil.

Validation of this simulation was carried out by simulating the results of previous experimental research and comparing them with the simulation results with the

same pre-processing, the configuration will be used in simulation process of this research. The experimental data used was taken from the journal Talukdar, Parag K., et al [11].

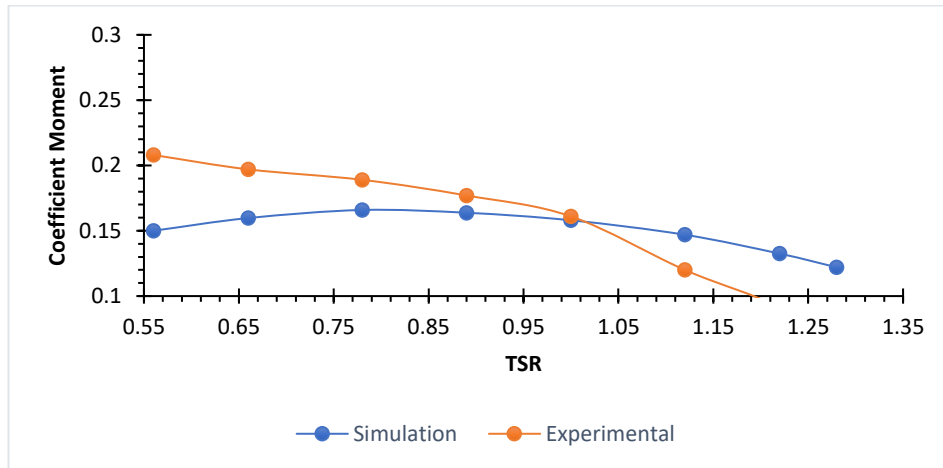


**Figure 9** Graphic coefficient moment simulation and experiment

From the graphic we know in low TSR value the CM of simulation is lower than CM of experiment, this happens especially in 3D model simulation, but when the TSR value is increased, the different of CM simulation and CM experiment will be smaller and the CM simulation will be above of CM experiment [12].

## 4. RESULT AND DISCUSSION

### 4.1 Turbine Performance

From the simulation results, it can be seen that the torque obtained at various rotational speeds and compared with the hydraulic power available for each turbine according to equation 2.15 is 6.86 kW. From the simulation results, performance data is obtained as follows

**Table 4.1** Turbine performance table at placement position one

TSR	rotational speed (rad/s)	C = 100 mm			C = 209 mm			C = 314 mm		
		Moment	Power (Watt)	Efficiency (%)	Moment	Power (Watt)	Efficiency (%)	Moment	Power (Watt)	Efficiency (%)
1.5	5.803	42.60	247.20	3.60	80.96	469.79	6.85	0.46	2.65	0.04
1.7	6.577	64.46	423.95	6.18	87.59	576.05	8.40	-78.76	-517.96	-7.55
2	7.737	101.15	782.64	11.41	50.13	387.89	5.65	-233.79	-1808.89	-26.37
2.2	8.511	108.37	922.29	13.44	0.37	3.16	0.05	-350.53	-2983.33	-43.49
2.5	9.671	99.88	965.98	14.08	-124.90	-1207.99	-17.61	-536.42	-5187.86	-75.62

**Table 4.2** Turbine performance table at placement position two

TSR	Rotational speed (rad/s)	C = 100 mm			C = 209 mm			C = 314 mm		
		Moment	Power (Watt)	Efficiency (%)	Moment	Power (Watt)	Efficiency (%)	Moment	Power (Watt)	Efficiency (%)
1.5	5.803	44.28	256.92	3.75	96.89	562.24	8.20	42.03	243.91	3.56
1.7	6.577	49.79	327.45	4.77	93.51	614.97	8.96	-26.09	-171.60	-2.50
2	7.737	103.73	802.59	11.70	93.14	720.64	10.50	-167.18	-1293.45	-18.85
2.2	8.511	115.43	982.37	14.32	59.14	503.31	7.34	-283.32	-2411.26	-35.15
2.5	9.671	135.39	1309.38	19.09	-23.42	-226.55	-3.30	-469.79	-4543.47	-66.23

From the table above we can see the turbine performance data for the two different placement positions with variations in chord length and in TSR conditions of 1.5 to 2.5, The following is an graphic of changes in turbine performance for each chord variation at two different placement positions in the tail race of the Bakaru Hydroelectric Power Plant.

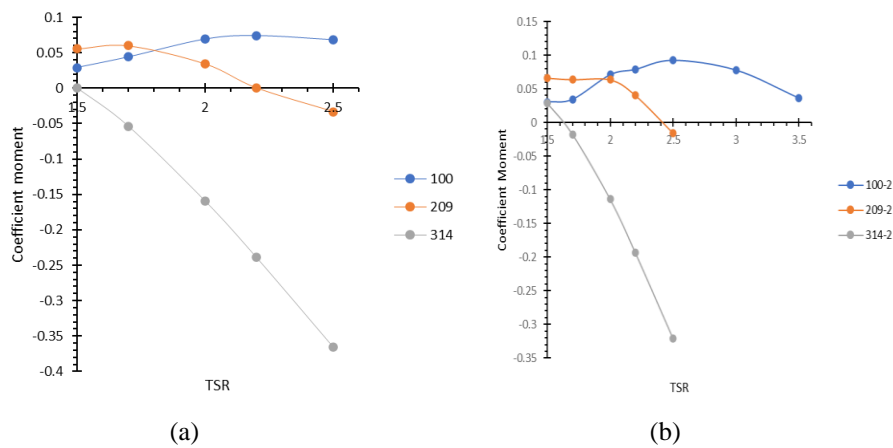


**Figure 10** Cp turbine for position 1 (a) and position 2 (b) in tail race with chord length variation

Based on the graph above, it can be seen that the turbine in the second position has a higher Cp compared to the turbine in the first position with the same chord length. And if we compare the three chord length variations, the turbine with a chord length of 100 mm has the highest Cp value, which are 0.23 at TSR 2.5. For the longest chord, the Cp value when the TSR is 1 is minus and continues to decrease as the TSR increases.

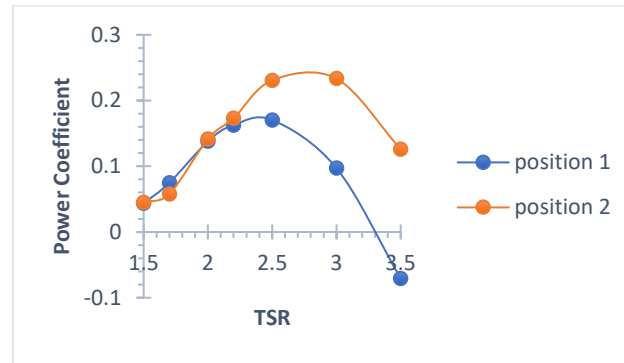


**Figure 11** Cp turbine with 100 mm chord length in different positions

## 4.2 Velocity Analysis

The velocity of the turbine with a chord length of 100 mm at TSR 2.5 conditions can be seen in Figure 12 below. From that we can see the fluid when passing through the barrier in tail race outlet make an increase in flow velocity, causing the flow velocity at position 2 to be higher than the flow at position 1. It can also be seen that the flow velocities which are passed the turbine are decrease, this can be seen from the contour color changing from blue light to dark blue. Apart from that, along the canal there is still a speed flow marked in light blue so that several turbines can still be added to maximize energy utilization in the 6 m wide tail race.

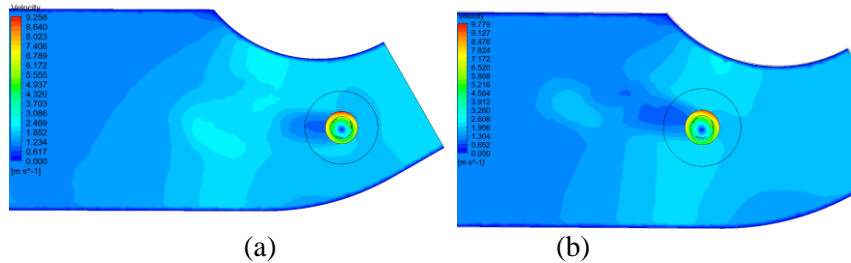


**Figure 12** Velocity contour of turbine with chord length 100 mm in position one (a) and position two (b) at TSR 2.5

The Figure 13 shows a simulation of fluid flow around the turbine with the velocity vector and color velocity distribution as the main indicators of the simulation results. Red and yellow colors indicate higher flow velocities (close to 9.25 m/s) while blue and green colors depict areas with lower velocities, especially behind the turbine (wake area or turbulence trail). This decrease in speed is caused by the interaction between the fluid flow and the turbine, which results in the extraction of fluid energy by the turbine to produce power.

Barriers can speed up flow in some areas (nozzle effect), but also slow down flow in other areas. The second position allows utilization of faster flow, but with increased turbulence. In contrast, the first position has a more stable flow with a more even speed distribution.

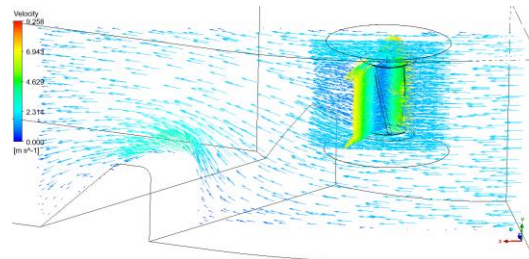


**Figure 13** Velocity Stream line in tail race

### 4.3 Pressure Analysis

From pressure contour of simulation results. There is no significant color change before and after the flow passes through the turbine, which indicates that there is no significant change in pressure in the tail race flow after it hits the turbine. Pressure changes only occur on the surface of the turbine blade due to impact with the turbine blade. This also shows the turbine does not use a pressure head to drive the turbine.

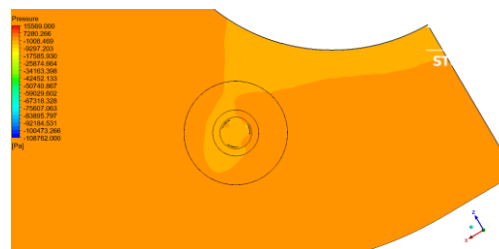


**Figure 14** Pressure contour in turbine with 100 mm chord length at position two

### 4.4 Benefit of Combined Cycle hydropower system in Bakaru HEPP

In HEPP there are two KPI (keys performance index) which are perform the production, there is CF (capacity factor) and PS (self-consumption). With maximize utilizing the HDKT in tail race we can produce electriciricity power of 48,56 kW (theoretical power) or if the max debit is 60% probility in a year, the annual HDKT production is 255,272.16 kWh. It will increase the annual CF of Bakaru HEPP 0.038.

## 5. CONCLUSION

The hydrokinetic turbine was designed for installation in the tail race of the Bakaru Hydroelectric Power Plant (HEPP) to enhance the system's energy efficiency through a combined-cycle hydropower approach. The conclusion of this research is:

Potential Power Generation from the theoretical potential of 48,56 kW that can be harnessed using hydrokinetic turbines, leveraging water flow with a mean velocity of 1,9 m/s in the tail race outlet as mean velocity which has been known from measurement with ADPC (Acoustic Doppler Current Profiler).

From Various configurations, including chord length and positioning, were analyzed using Computational Fluid Dynamics (CFD) simulations. The optimal configuration yielded a maximum power coefficient ( $C_p$ ) of 0,23 at a Tip Speed Ratio (TSR) of 2,5 in position 2.

The generated energy could be utilized to reduce the self-consumption (PS) of Bakaru HEPP, enhancing its overall capacity factor by an estimated 0,038%, contributing to a more sustainable operation in line with Net Zero Emission (NZE) goals.

The utilization of HDKT in tail race Bakaru HEPP can effectively increase the energy output of a conventional hydropower system without major structural modifications.

## Acknowledgement

Thanks to Faculty of Mechanical and Aerospace Engineering at Institut Teknologi Bandung for their support and resources in conducting this research. Special thanks are extended to the team at the Bakaru Hydroelectric Power Plant for providing valuable data and insights on site-specific conditions. We also acknowledge the financial and technical assistance from PLN NP (Perusahaan Listrik Negara Nusantara Power), which made this study possible. Finally, we thank all colleagues and collaborators who contributed feedback and expertise, greatly enhancing the quality and scope of this research.

## References

- [1] A. Demirbas, “Global renewable energy projections,” *Energy Sources, Part B: Economics, Planning and Policy*, vol. 4, no. 2, pp. 212–224, 2009, doi: 10.1080/15567240701620499.
- [2] EIA, “Electric Power Annual,” *Eia.Doe.Gov*, vol. 0348, no. January, p. 2, 2022.
- [3] IHA, “Hydropower Status Report 2020,” *International Hydropower Association*, p. 52, 2022.
- [4] A. M. Vicedo-Cabrera *et al.*, “Temperature-related mortality impacts under and beyond Paris Agreement climate change scenarios,” *Clim Change*, vol. 150, no. 3–4, pp. 391–402, 2018, doi: 10.1007/s10584-018-2274-3.
- [5] E. Quaranta and S. Muntean, “Wasted and excess energy in the hydropower sector: A European assessment of tailrace hydrokinetic potential, degassing-methane capture and waste-heat recovery,” *Appl Energy*, vol. 329, Jan. 2023, doi: 10.1016/j.apenergy.2022.120213.
- [6] “Turbulence\_Modeling\_For\_Beginners”.
- [7] R. Kumar and S. Sarkar, “Effect of design parameters on the performance of helical Darrieus hydrokinetic turbines n,” *ScienceDirect*, 2022, doi: <https://doi.org/10.1016/j.rser.2022.112431>.
- [8] C. R. Wright and M. C. Hansen, “OPTIMIZATION OF HELICAL TURBINE IN LOW HEAD APPLICATIONS,” 2011.
- [9] I. Bel Mabrouk and A. El Hami, “Effect of number of blades on the dynamic behavior of a Darrieus turbine geared transmission system,” *Mech Syst Signal Process*, vol. 121, pp. 562–578, Apr. 2019, doi: 10.1016/j.ymssp.2018.11.048.
- [10] B. D. Adhikary, P. Majumdar, and M. Kostic, “CFD Simulation of Open Channel Flooding Flows and Scouring Around Bridge Structures.”
- [11] P. K. Talukdar, S. Kumar, V. Kulkarni, A. K. Das, and U. K. Saha, “On site testing of a zero head vertical axis helical water turbine for power generation,” in *ASME 2015 Gas Turbine India Conference, GTINDIA 2015*, American Society of Mechanical Engineers, 2015. doi: 10.1115/GTINDIA2015-1230.
- [12] “Optimization and analysis of self-start... turbine pairs\_ A CFD-Taguchi approach (1)”.